TABLE 2: Elemental Analyses (%)

Compound	Calculated C	H	N	P	Found C	H	N	P	Mole wt.	Remarks
I	36.97	5.49	19.90		36.88	5.60	19.75		422.35	$1H_2O$
II	38.46	6.24	17.94	6.61	38.61	6.25	17.85	6.31	468.42	$2H_2O$
III	27.92	3.01	13.96	5.14	27.80	3.05	14.00	5.24	602.21	$2Na^+$
IV	19.55	2.81	9.77		19.34	2.92	9.76		860.20	$4Na^+$ $3H_2O$
V	41.53	7.21	13.36		41.47	7.09	13.20		838.72	$2TEA^+$ $2H_2O$
VI	50.25	8.84	15.13		49.98	8.91	15.20		740.87	$2TEA^+$ $2H_2O$
VII	28.37	4.39	10.45	11.55	28.40	4.40	10.50	11.60	804.44	$4Na^+$ $3H_2O$
VIII	41.15	6.63	17.28		41.08	6.57	17.37		729.68	$2NH_4^+$ $4H_2O$
IX	43.03	6.67	17.37		43.27	6.78	17.32		725.69	$2NH_4^+$ $3H_2O$
X	42.79	6.92	16.64		42.59	6.95	16.78		757.73	$2NH_4^+$ $4H_2O$
XI	36.49	6.85	22.53		36.41	6.83	22.37		559.52	$2NH_4^+$ $2H_2O$
XII	37.69	7.03	21.98		37.47	7.12	21.86		573.55	$2NH_4^+$ $2H_2O$
XIII	38.84	7.21	21.46		38.69	7.18	21.40		587.58	$2NH_4^+$ $2H_2O$
XIV	28.54	5.39	11.65	3.68	28.46	5.44	10.50	3.29	841.48	$2Na^+$ $8H_2O$
XV	31.47	4.90	12.23		31.23	4.88	12.21		801.44	$2Na^+$ $4H_2O$
XVI	24.68	3.62	10.07		24.53	3.58	9.99		973.35	$4Na^+$ $3H_2O$
XVII	27.02	3.35	10.51	9.96	27.05	3.38	10.54	9.93	933.34	$4Na^+$

iodoacetate to N^6-aminoacyl derivatives of AMP was carried out without difficulty, and the paper chromatogram was developed in solvent system C (see Table 1) and the band at R_B 0.37–0.38 was further eluted with water at 4 °C.

Elemental analyses for the Compound II, III, VII, XIV, and XVII were performed by Galbraith Labs, Inc., Organic Microanalyses, Knoxville, TN, U.S.A., and others were determined with C, H & N Analyzer, Hewlett Packard, Model 185B.

The fractional collections were used with Fractomette Alpha 200 Fraction collector (Buchler) 115V 60HZ, 3 m*l* per min., and collected 12 m*l* per each tube.

References

(1) A. Lehninger, Biochemistry, "Molecular basis of cell structure and function", 2nd Ed., New York, Worth, 1975, p. 309-333.

(2) F. Kappler and A. Hampton, *J. Org. Chem.*, **40**, 1378 (1975).

(3) L. Goodman and A. Gilman, "Pharmacological basis of therapeutics", 5th Ed., London, Macmillan, 1975, p. 1248-1307.

(4) J. Dipalma, "Drill's pharmacology in medicine", 3rd Ed., New York, McGraw-Hill, 1964, p. 1231-1242.

(5) A. Hampton, L. Slotin and R. Chawla, *J. Med. Chem.*, **19**(11), 1279 (1976).

(6) D. Hoard and D. Ott, *J. Amer. Chem. Soc.*, **87**, 8, 1785 (1965).

(7) J. Kozarich, C. Chinault and S. Hecht, *Biochemistry*, **12**, 22, 4458 (1973).

(8) Partial work for this paper was done while the author was a research fellow of the Institute for Cancer Research, Philadelphia, U.S.A in 1975. However, for this paper, the author repeated the procedure for perfection.

The Vacancies-in-Solid Model Applied to Molar Volumes and Isothermal Compressibilities of Solid Krypton and Xenon

Seuk Beum Ko

Department of Chemistry Education, Jeonbug National University, Jeonju 520, Korea

Wan Kyue Kim

Department of Chemical Engineering, Soongjun University, Seoul 151, Korea

(Received August 28, 1980)

The molar volumes and the isothermal compressibilities of solid krypton and xenon are calculated using the vacancies-in-solid model. The central pairwise additive (Mie-Lennard-Jones 12,6) potential in a uniform potential field is used. The results are compared with the other theoretical results and the available experimental values.

Introduction

The equation of state of rare gas solids has been studied by a number of workers. Most theoretical studies[1-6] on thermodynamic properties of rare gas solids have been done for perfect crystals. Among these, Born[7], Horton[8] and Cupta[9] have derived an equation of state of the rare gas solids applying a two-body central force and a harmonic lattice vibration to the perfect crystal structure. Their results are all in good agreement with observed data at very low temperatures ($T \leqslant \theta_0/5$). However a large discrepancy between theoretical and experimental data is generally observed at high temperatures ($T \geqslant \theta_0/2$) and it becomes larger with increasing temperatures. Zucker[10] studied theoretically the thermodynamic properties of solid argon using an Einstein model modified to include anharmonic effects. The anharmonic Einstein model for solid argon gives better agreement with experiment at low temperatures, but generally a large discrepancy between the anharmonic values and the observed values is observed at higher temperatures. For $T \geqslant 0$ °K the Helmholtz free energy of a real crystal has a minimum for the arrangement where a certain fraction of the lattice sites are unfilled. From the differences[11-20] between the bulk properties and the X-ray data of vacancy-free crystals it is found that the dominant thermal defect in close packed crystals is the atomic vacancy. The bulk properties of rare gas solids have been compared with the X-ray data. The mole fractions of vacancies, and enthalpies and entropies of vacancy formation for solid neon, argon and krypton have been estimated from the analyses of bulk properties and X-ray data. Hall[21] and Kanzaki[22] theoretically studied the enthalpy of formation of vacancy. In view of the above, we think it is worthwhile to investigate the vacancy defect effects on the thermodynamic properties of the monatomic crystals by considering lattice vacancy defects in the canonical ensemble partition function. Such a study will furnish a useful information about the crystal structure for these solids. In earlier papers[23,24] we have derived a solid partition function for monatomic crystals, taking account of lattice vacancy defects and two maximum phonon frequencies for perfect crystals, and studied the vapor pressures of solid argon and xenon, using a Mie-Lennard-Jones 12,6 potential in a uniform potential field. In this paper we have used the same vacancies-in-solid model to the molar volumes and isothermal compressibilities of solid krypton and xenon which have the small effect of the zero-point vibration energy on their crystalline physical properties. And also, we have discussed the method of determination of the potential parameters in our calculations. Finally, we have evaluated our theoretical molar volumes and isothermal compressibilities from 0 °K to the triple point, and compared our results with other theoretical calculations and the available experimental data.

Theory

According to the vacancies-in-solid model,[23,24] the cannonical ensemble partition function $Q(N, V, T,)$ for the monatomic crystals is

$$Q(N,V,T) = [q(l, T)]^{xN}[q(m, T)]^{(1-x)N}\frac{(N + N_h)!}{N!\,N_h!} \quad (1)$$

with

$$x = V_0/V$$

where x is a probability that a central atom finds atoms at its first neighboring coordination sites. V_0, V, N and N_h are the molar volume at 0 °K, the molar volume at a given temperature, the number of atoms, and the number of vacancies, respectively. $q\ (1, T)$ is the molecular partition function assigned to the atom surrounded entirely by atoms with the maximum probability finding atoms, and $q(m, T)$, assigned to the atom with the minimum probability. Therefore we may consider the solid partition function as consisting of x mole fraction of perfect crystal-like part and (1-x) mole fraction of imperfect crystal-like part together with a configurational part. The molecular partition function for the perfect crystal-like part is as follows:

$$q\ (1, T) = \left(2\sinh\frac{\theta_C}{2T}\cdot 2\sinh\frac{\theta_D}{2T}\right)^{-3/2}\exp\left(-\phi_C/kT\right)$$

where θ_D is the Debye temperature, and θ_C is given in order of (4/7) θ_D. ϕ_C is the static potential energy per atom of the perfect crystal-like part. Since an imperfect crystal-like part contains lattice vacancies within it, an imperfect oscillator shall be able to make either an atom-vacancy link or atom-atom link, each corresponding to β- or α-state. Thus the imperfect oscillator exists in either state of the two. On the basis of the ordinary statistical expression for isomeric degenerate state, the partition function $\beta(m, T)$ of an imperfect oscillator is expressed in terms of the sum of the partition function of α-state and β-state imperfect oscillator as follows:

$$q\ (m,\ T) = q_\alpha\ (1,\ T) + q_\beta(x,\ T)$$

The partition function of the imperfect oscillator in α-state (q_α) may be approximately equalized to that of a perfect oscillator.

$$q_\alpha\ (1,\ T) = q\ (1,\ T)$$

On the contrary, the imperfect oscillator in β-state makes an atom-vacancy link due to the presence of a vacancy next to itself, hence it has only lower frequency and higher potential energy that those of the perfect oscillator. Therefore the partition function of the imperfect oscillator in β-state, q_β,

is given as follows:

$$q_\beta(x, T) = g_n \left[2\sinh\frac{\theta_C}{2T}\right]^{-3} \exp(-\phi_n/kT)$$

g_n is assigned to a positional degeneracy factor related to the number and kinds of vacancies and the geometric structure of a crystal. In the case of vacancy defect crystals. The number of lattice vacancy is so small as to make it improbable that two vacancies on the average occupy neighbouring sites, so that it is natural for us to assume only existence of a mono-vacancy around a given central atom. g_n is assumed to be equal to 1. ϕ_n is the static potential energy of β-oscillator. We assume that perfect oscillators are subjected to the Mie-Lennard-Jones 12,6 potential in the uniform field strength. Thereby, the static potential energy ϕ_c of perfect oscillators will be given by the following expression.

$$-\Phi_c(x) = -N\phi_c(x) = U_e + D_e\left[2(a_0/a)^6 - (a_0/a)^{12}\right]$$
$$= U_e + D_e(2x^2 - x^4)$$

with

$$x = (a_0/a)^3 = V_0/V$$

where a_0 and a are the equilibrium distances between two atoms at 0 °K and a given temperature, respectively. U_e is the minimum potential energy in the uniform potential strength, and D_e is the dissociation energy required to separate stable atomic pairs far apart to infinitive distance in the uniform field. The potential energy of an imperfect oscillator in β-state is assumed to be given as follows:

$$\phi_\beta = \phi_c + \epsilon_0$$

where ϵ_0 is the difference of the static potential energy per atom between the perfect oscillator and an imperfect oscillator in β-state.

Then

$$E_0 = N\epsilon_0$$

and

$$E_0 = -(\Phi_c - \Phi_\beta)$$

The Helmholtz free energy of a crystal is given as

$$A = -\Phi_c + A_{deg.} + A_{conf.} + A_{vibr.}$$

where each term is given as

$$-\Phi_c = U_e + D_e(2x^2 - x^4)$$

$$A_{deg.} = -RT(1-x)\ln(1+\Delta) \quad \text{with} \quad \Delta = q_\beta/q_\alpha$$

$$A_{conf.} = -kT\ln[(N+N_h)!/N!N_h!]$$

$$A_{vib.} = \frac{3}{2}RT\ln\left(2\sinh\frac{\theta_C}{2T}\cdot 2\sinh\frac{\theta_D}{2T}\right)$$

where Φ_C is the static lattice energy, $A_{conf.}$, $A_{deg.}$ and $A_{vibr.}$ are called configurational, degenerate and vibrational Helmholtz free energy, respectively. The thermodynamic pressure (P) of a crystal is equal to the negative isothermal volume derivative of the Helmholtz free energy A. Hence, the equation of state, which connects the state parameters, P, V and T of a solid, is

$$P(V, T) = P_{sl.}(V) + P_{conf.}(V, T) + P_{deg.}(V, T) + P_{vib.}(V, T) \quad (3)$$

where each term is given as follows.

$$P_{sl.}(V) = -(4D_e/T)(1-x^2)x^2$$

$$P_{conf.}(V, T) = -\frac{RT}{V}[\ln(1-x)/x]$$

$$P_{deg.}(V, T) = \frac{RT}{V}[x\ln(1+\Delta)]$$

where $P_{sl.}$, $P_{conf.}$, $P_{deg.}$ and $P_{vibr.}$ are called static, configurational, degenerate and vibrational pressure, respectively, and the vibrational pressure is assumed to be negligible, *i.e.* the vibrational frequency is assumed to be independent on the volume of a crystal. Isothermal compressibility (χ_T) was found using the relation.

$$1/\chi_T = kTV(\partial^2 \ln Q/\partial V^2)$$

The following expression are obtained

$$\chi_T = \chi_{sl.}(V) + \chi_{conf.}(T, V) + \chi_{deg.}(T, V)$$

here

$$\chi_{sl.} = 1/\left(\frac{RT}{V_0}\right)\left[\frac{4D_e}{RT}(5x^2 - 3)x^3\right]$$

$$\chi_{deg.} = 1/\left(\frac{RT}{V_0}\right)[2x^2\ln(1+\Delta)]$$

$$\chi_{conf.} = 1/\left(\frac{RT}{V_0}\right)[x/(1-x)]$$

where $\chi_{sl.}$, $\chi_{conf.}$ and $\chi_{deg.}$ are called static lattice, configurational and degenerate isothermal compressibility, respectively.

Results

Parameters of the Mie-Lennard-Jones potential, we make use of the Mie-Lennard-Jones potential (12, 6 potential) in the uniform field strength. The potential parameters D_e and U_e are determined by solving the equation of state for the solid and the equation of sublimation pressure, using the observed triple point properties, *i.e.* the triple point temperature, the sublimation pressure and the molar volume at triple point, and the molar volume at 0 °K, and the Debye temperature. We have recent crystal data for the determinations of potential parameters. The observed crystal data for xenon

and krypton have been taken from the review book of Klein.[6] The used experimental input data and the obtained potential parameters thus are presented in Table 1. In Table 1, E_0 are obtained by using the Debye temperature and the triple point temperature from the following condition of fusion; At triple point temperature, the probabilities of imperfect oscillator, either in α-state or in β-state, are equal *i.e.*, $q_\alpha = q_\beta$.

TABLE 1: Experimental Input Data for Potential Parameter Determinations and Potential Parameters Estimated

Input date	Kr	Xe
Thermodynamic Debye temperature (°K)	63[a]	55[a]
Triple point temperature (°K)	115.763[d]	161.39[b]
Sublimation pressure at triple point (torr)	547.5[d]	612.2[d]
Molar volume at triple point (cc/mole)	30.013[d]	38.59[c]
Molar volume at 0 °K (cc/mole)	27.098[d]	34.74[d]
Parameters estimated		
c (°K)	36	31
E_0 (cal/mole)	195.96	277.35
D_e (cal/mole)	1225.1	1661.2
U_e (cal/mole)	1605.8	2268.5

[a]Ref. 3, [b]ref. 26, [c]ref. 30, [d]ref. 6.

Molar Volumes. The equation of state for the solid is rearranged to evaluate molar volumes at a series of temperatures as follows

$$4D_e/RT = [1/x^2(1-x^2)][-\frac{1}{x}\ln(1-x) + \ln(1+\Delta) - PV/RT]$$

By a trial and error method, we may obtain the $\chi(T)$ values for given temperatures, then a molar volume (V) for a given temperature is estimated from the molar volume (V_0) at 0 °K since $\chi(T) = V_0/V$.

Thus the calculated results of molar volumes for krypton are shown in Figure 1 along with recent experimental data for comparison, and for xenon in Figure 2. The experimental molar volumes for krypton are taken from X-ray measurements of Losee *et al.*[14c] at $T \leqslant 80$ °K and the bulk data of Korpiun *et al.*[27] at $T > 80$ °K. The observed molar volumes for xenon have been taken from X-ray measurements of Sears *et al.*[28,29] at $T \leqslant 120$ °K, and pycnometric measurements of Gavrilko *et al.*[30] at $T > 120$ °K. The experimental error of bulk data has been given to be ±5 percent. The theoretical molar volumes of Gupta *et al.*[9] for krypton and xenon are also given in Figure 1 and 2 for comparison.

Isothermal Compressibility. In calculations of isothermal compressibility, the value of the molar volume found already were used. The calculated results for solid krypton and xenon

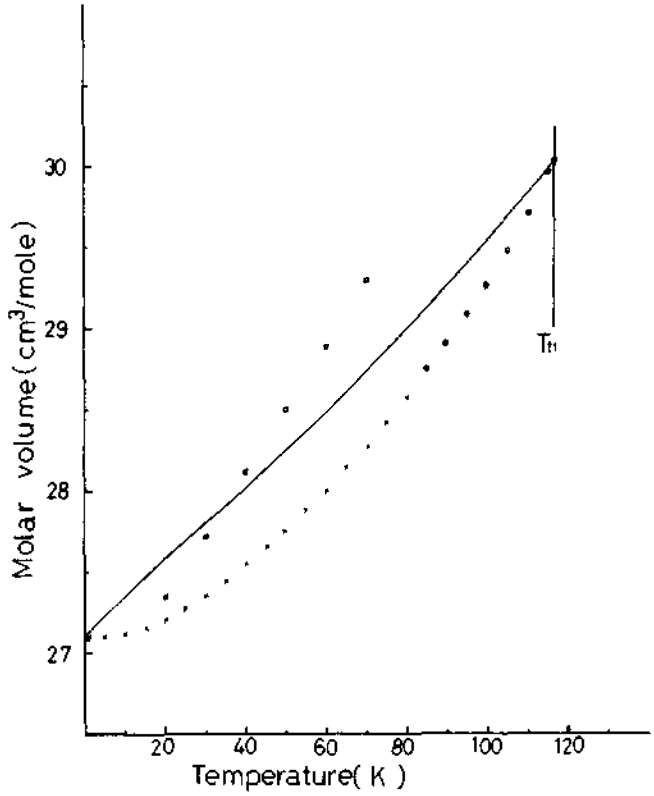

Figure 1. Molar volume-temperature curve for solid krypton. Crosses: obtained from X-ray measurements by Losee *et al.*[14c]. Open circles: bulk data of Korpiun *et al.*[27]. Squares: theoretical values of Gupta *et al.*[9]

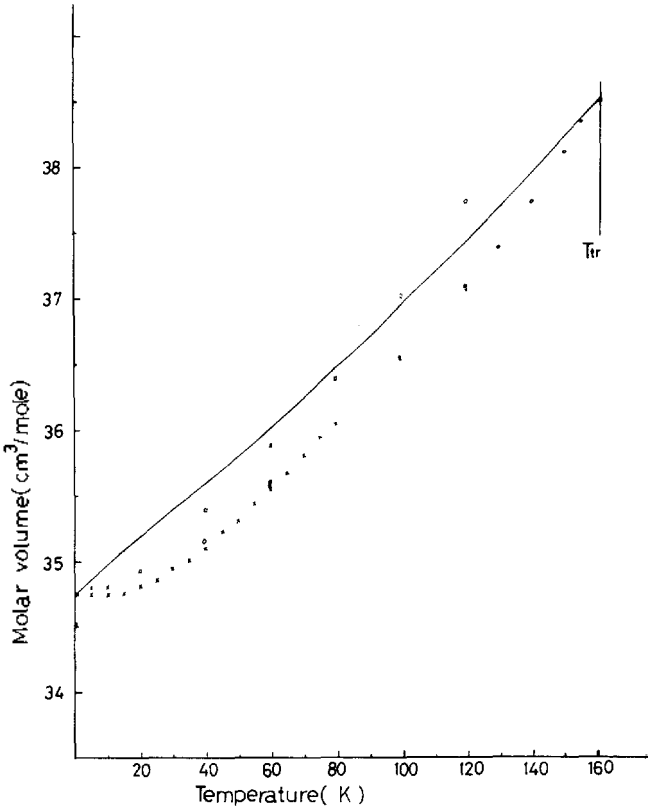

Figure 2. Molar volume-temperature for solid xenon. Crosses: obtained from X-ray measurements by Sears *et al.*[28,29]. Open circles: obtained from pycnometric measurements by Gavrilko *et al.*[30]. Squares: theoretical values of Gupta *et al.*[9]

are presented in Figures 3 and 4 along with observed values for comparison, respectively. Korpiun *et al.*[27] have measured isothermal compressibility with the optical dilatometer from 4.2 °K to 115 °K in solid krypton while Losee *et al.*[14c,31] have measured isothermal compressibility using the X-ray diffraction technique. Swenson *et al.*[25,32] have measured isothermal compressibility with piston displacement method from 0 °K to the triple point in solid xenon while Bezuglyi *et al.*[33] have measured isothermal compressibility with the ultrasonic velocity measurements. Error of X-ray isothermal compressibility for krypton was estimated to be ±1 % at 4 °K, rising to ±3 % at 78 °K, to ±5 % at T = 90 °K, and to about ±10 % at higher temperatures. But the error in the optical dilatometer measurements was estimated to be less than ±1 percent. For the piston displacement isothermal compressibility of xenon, error was estimated to range from ±6 % at 202K to ±13 % at 150 °K. The theoretical isothermal compressibilities of Barron and Klein[34] for krypton and xenon are also given in Figures 3 and 4 for comparison.

Discussions

The X-ray diffraction method and the bulk method have been applied in determining the molar volumes of solids. At higher temperatures, *i.e.* $T>70$ °K for Kr and $T>120$ °K for Xe, recrystallization effects enlarged the grains and the line structure on the photographic plates became spotty. It is difficult, therefore, to use X-ray diffraction methods in the higher temperature region. The bulk method is preferably used in determining the molar volumes in the higher temperature region. The results of both measurements agree in the lower temperature region, *i.e.* at $T<80$ °K for krypton and at $T<120$ °K for xenon within experimental errors. But bulk density is somewhat less than X-ray density at $T<80$ °K for Kr, and at $T<120$ °K for xenon, and decreases more rapidly with temperature than X-ray density ρ_x. It should be noted that the bulk density measurements are especially sensitive to crystal defects and X-ray measurements give the X-ray densities of vacancy-free crystal. The difference between both density may be only explained by the thermal creation of vacancies. If the crystal contains N_h vacancies and N atoms, and each vacancy occupies a lattice site, the following relation is given between the bulk volume (density) V and the X-ray volume (density) V_x

$$\frac{N_h}{N+N_h} = \frac{V-V_x}{V} = \frac{\rho_x-\rho}{\rho_x} = C \qquad (5)$$

The equation (5) is the essence of the methods of determining the mole fraction (c) of vacancy at a given temperature, and only useful when the solid contains a high concentration of vacancies. Using the equation (5), vacancy mole fraction

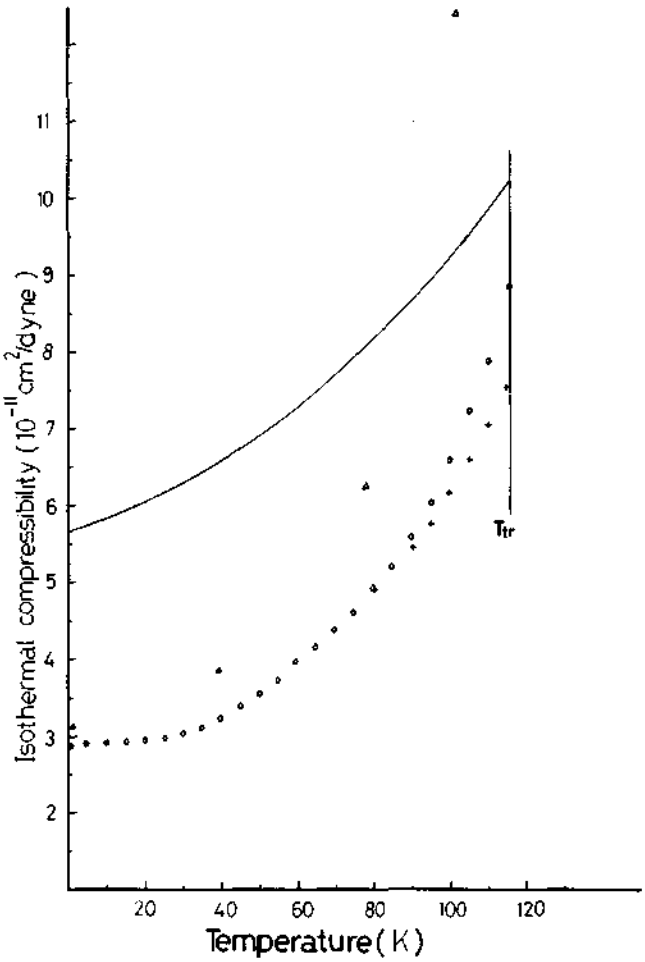

Figure 3. Isothermal Compressibilities for solid Krypton. Open circles: obtained from the optical dilatometer by Korpiun *et al.*[27] Crosses: X-ray data by Losee *et al.*[14c,31] Triangles: theoretical values of Barron *et al.*[34]

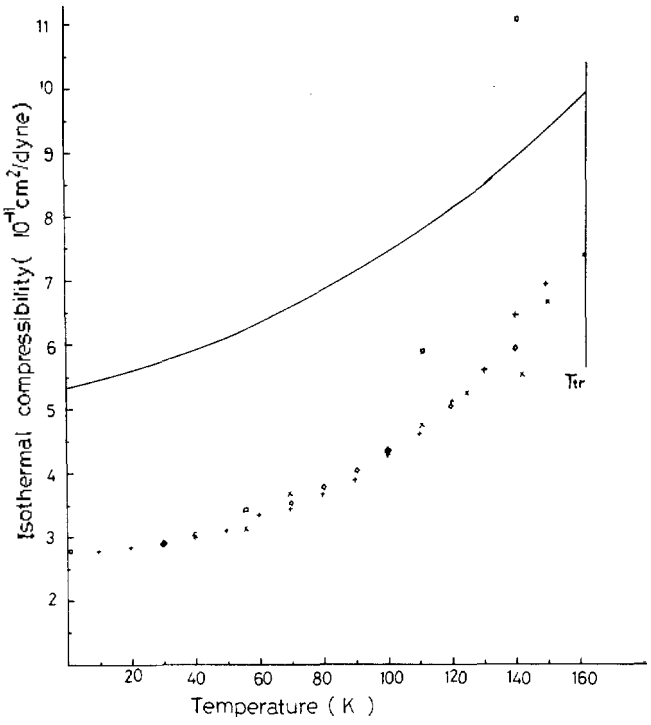

Figure 4. Isothermal compressibilities for solid xenon +: obtained from the ultrasonic velocity measurements of Bezuglyi *et al.*[33] Crosses and rhombohedra: obtained from the piston displacement method of Swenson *et al.*[25,32] Squares: theoretical values of Barron *et al.*[34]

measurements were available only for krypton near triple point, but not available for xenon, but it is found that the relative volume differences always yield positive values in spite of any aggregation of the vacancies into divacancies, trivacancies, *etc.* for rare gas solids. A typical value of the vacancy mole fraction for solid neon, argon, krypton, and xenon is found to be in order of about 10^{-3} near the triple point[6], consequently ρ and ρ_x would have to be measured to an accuracy of ±0.01 percent if the vacancy mole fraction is to be determined to an accuracy of about ±10 percent. This requirement of a very high accuracy is a serious limitation of the vacancy mole fraction measurements. Of the two densites ρ_x has been determined with the error of about ±0.005 percent, but the inherent uncertainties in bulk-density determinations are from 0.1 to 0.05 percent.[1] Therefore the experimental separation of vacancy contribution on the molar volume is quite difficult because of the experimental inaccuracy of bulk data and only limits on vacancy concentration can be set near the triple point. According to our theory, the vacancy mole fraction is given by the following expression, because the mole fraction of imperfect atoms is given by $(1-x)$ and each central atom is supposed to link itself to only one monovacancy occuping one of Z coordination sites.

$$C = \frac{1 - x}{Z} \tag{6}$$

Then the equilibrium mole fraction of monovacancy is thermodynamically related to the Gibbs free energy (g) for monovacancy formation by the following expression

$$C = e^{-g/kT} = e^{s/k}\, e^{-h/kT} \tag{7}$$

where h and s are the enthalpy and entropy of monovacancy formation. Using equations (6) and (7), the monovacancy mole fraction, and the enthalpy and the entropy of monovacancy formation were calculated near triple point and are presented in Table 2. Losee *et al.*[14,27] published a direct determinations of vacancy mole fraction and the enthalpy and the entropy of vacancy formation in krypton by comparing bulk length measurements with X-ray lattice parameter measurements, and their experimental results of analysis are as shown in Table 2. Enthalpies of vacancy formation were obtained by Glyde[35] from the calculations which include the zero-point energy, pair relaxation and the many-body dipole-dipole contribution for perfect crystals. The estimated enthalpy of monovacancy formation is in good agreement with the experimental value within experimental error. Calculated enthalpies of our present theory are more consistent with observed values than other theory. The experimental values of the entropy of monovacancy formation are subject to large uncertainties due to the fact that they are obtained by a long extrapolation of the graphs. Our calculated entropy for monovacancy formation fall nearly within the limits set by the experimental values. This fact seems to explain the validity of our theory. As shown in Figures 1 and 2, it is not surprising that the theoretical and the experimental molar volumes agree at 0 °K and triple point because the molar volumes at 0 °K and triple point are used in determining potential parameters. Triple point is in fact the only fixed point in determining potential parameters. The observed molar volumes are the bulk volumes near the triple point, *i.e.* at $T>70$ °K for Kr and at $T>120$ °K for Xe. Our estimated molar volumes closely approach bulk molar volumes with approaching the triple point, but with decreasing temperatures deviate more from observed volumes. Bulk volume is larger than X-ray volume in the higher temperature range. It can be seen that our theoretical molar volumes are somewhat higher than observed bulk volumes between 0 °K and triple point. Our results of molar volumes show a maximum discrepancy near about $T \leqslant T_t/2$. The maximum relative discrepancy of the molar volumes for the krypton and xenon is 1.7 and 1.5 %, respectively. But the present molar volumes calculated are in good agreement with observed values within experimental error. As shown in Figures 3 and 4, the present theoretical isothermal compressibilities of both krypton and xenon are higher than the observed values at the triple point by about 10 percent, but the triple point this difference is within experimental error. A more large discrepancy exists with decreasing temperatures. The large discrepancy at lower temperatures is considered to be due to an oversimplified model for the potential. As also seen in Figures 1, 2, 3 and 4, theoretical molar volumes of Gupta *et al.* and isothermal

TABLE 2: The Monovacancy Mole Fraction at Triple Point and the Enthalpy and the Entropy of Monovacancy Formation near Triple Point

	$C\times10^3$		s/k		h/k		
	Our theory	Experimental	Our theory	Experimental	Our theory	Experimental	Other theory
Kr	8.1	3.2[a]	3.8	2.0 $^{+1.0}_{-0.5}$[a]		896±101[a]	
		2.9[b]		2.8 $^{+0.8}_{-0.9}$[b]	998	999±101[b]	1237[d]
				3.0±0.5[c]		1070±95[c]	
Xe	8.4		3.7		1368	1248[d]	1766[d]

[a]Ref. 14, [b]ref. 27b, [c]ref. 27a, [d]ref.

compressibilities of Barron *et al.*[34] show somewhat better than our theory at low temperatures ($T<T/2$), but becomes by far worse than our theory with increasing temperatures. Gupta *et al.* calculated molar volumes on the basis of perfect crystal structure with (exp. 6) potential and an Einstein approximation of lattice vibration. Barron and Klein isothermal compressibilities on the basis of an anharmonic model with central interatomic forces (6–12 all neighbor potential model). Such a large discrepancy on Gupta's and Barron's values shows a general tendency to be found in all the theoretical values computed on the basis of perfect crystal structure. Perhaps this will be arised from the fact that they have taken no account of lattice vacancy in contrast with our present theory. While the present calculations show an agreement with the experimental results at temperatures approaching the triple point, there is greater discrepancy with decreasing temperature. At the higher temperatures, these agreement between theoretical and experimental data may be interpreted as justifying our present theory. The greater discrepancy at lower temperatures may be due to an oversimplified model for the potential of interaction among the atoms in the crystals, an overestimation of the configurational factor, and an ignorance of the volume dependence on the Debye temperature.

Conclusions

From the above discussions, we may say that the main frame of our present theory is at least in a right sign and a right magnitude. Thus we may deduce some conclusion from our present results as follows.

1. Although a perfect crystal exists at considerably low temperatures, it is required that the complete discription of solid state takes account of the presence of vacancy defects, since it has been found from our present theory that the present theoretical molar volumes of solid krypton and xenon are in good agreement with observed values within experimental error. This fact is also supported by analysis of experimental heat capacity[36] and density.[11-20]

2. Ordinary equation of state of the solid based upon standard lattice theories involve pressures expressed in terms of the sum of the static pressure and vibrational pressure which is ignored by our model. Our model, however, indicates that the contribution of the configurational and isomeric degenerate pressure are more of importance, at least, near triple point rather than that of vibrational pressure, since, in spite of the fact that the vibrational pressure was neglected, theoretical estimates of solid volumes are in good agreement with observed data within experimental error.

3. The magnitude of anharmonicity contribution on thermodynamic properties is not as great as what other workers have mentioned.

References

(1) G. L. Pollack, *Rev. Mod. Phys.*, **36**, 748 (1964)

(2) E. R. Dobbs and G. O. Jones, *Rept. Progr. Phys.*, **20**, 516 (1957).

(3) A. C. Hollis Hallet, "Argon, Helium, and the Rare Gases", Ed. G. A. Cook, Vol 1, John Wiley and Sons Inc., N.Y., 1961, p. 313.

(4) G. Boato, *Cryogenics*, **4**, 65 (1964).

(5) G. K. Horton, *Amer. J. Phys.*, **36**, 93 (1968).

(6) M. L. Klein and J. A. Venables, "Rare Gas Solids", Vol. 1 (1976) and 2 (1977) Academic Press, New York.

(7) M. Born and K. Huang, "The Dynamical Theory of Crystal Lattices", Oxford University Press, London, 1954.

(8) G. K. Horton, and J. W. Leech, *Proc. Phys. Soc.*, **82**, 816 (1963).

(9) N. P. Gupta and B. Dayal, *Phys. Stat. Sol.*, **18** 731 (1966) **20**, 321 (1967); **21**, 661 (1967).

(10) I. J. Zucker, *Phil. Mag.* **3**, 987 (1958).

(11) O. G. Peterson, D. N. Batchelder, R. O. Simmons, *Phys. Rev.*, **150**, 703 (1966).

(12) B. L. Smith and J. A. Chapman, *Phil. Mag.*, **15**, 739 (1967).

(13) M. Van Witzenburg, *Phys. Lett.*, **25A**, 293 (1967).

(14) (a) D. L. Losee and R. O. Simmons, *Phys. Rev. Lett.*, **18**, 451 (1967); (b) *Phys. Rev.*, **172**, 934 (1968); (c) **172**, 944 (1968).

(15) R. G. Pritchard and D. Gugan, *Phys. Lett.*, **32A**, 124 (1970).

(16) P. M. Bronsveld, S. K. Kunra and J. C. Stryland, *Bull. Amer. Phys. Soc.*, **16**, 63 (1971).

(17) W. E. Schonecht, Ph.D. Thesis, University of Illinois (1971).

(18) L. A. Schwalbe, Ph.D. Thesis, University of Illinois (1973).

(19) P. Korpiun and H. J. Coufal, *Phys. Stat. Sol.*, (a) 6,187 (1971)

(20) R. K. Crawford, W. F. Lewis and W. B. Daniels, *J. Phys. C.*, **9**, 1381 (1976).

(21) G. L. Hall, *J. Phys. Chem. Solids*, **3**, 210 (1957).

(22) H. Kanzaki, *J. Phys. Chem. Solids*, **2**, 24 (1957).

(23) W. K. Kim, Soong-jun Univ. Press, 6, (1976).

(24) S. B. Ko, Jeon Bug National University, *Basic Science Review*, **2**, 87 (1979).

(25) M. S. Anderson and C. A. Swenson, *J. Phys. Chem. Solids*, **36**, 145 (1975).

(26) D. R. Lovejoy, *Nature*, **197**, 353 (1963).

(27) (a) H. J. Coufal, R. Veith, P. Koupiun and E. Lüscher, *J. Appl. Phys.*, **41**, 5082 (1970); (b) P. Korpiun and H. J. Coufal, *Phys. Stat. Sol.*
(a) **10**, 187 (1971); (c) H. J. Coufal, R. Veith, P. Korpiun and E. Lüscher, *ibib.*, **38**, K127 (1970).

(28) D. R. Sears and H. P. Klug, *J. Chem. Phys.*, **37**, 3002 (1962).

(29) A. J. Eatwell and B. L. Smith, *Phil. Mag.*, **6**, 41 (1961).

(30) V. G. Gavrilko and V. C. Manzhelii, *Sov. Phys. Solid State*, **6**, 1734 (1965).

(31) A. O. Urvas, D. L. Losee and R. O. Simmons, *J. Phys. Chem. Solids*, **28**, 2269 (1967).

(32) J. R. Packard and C. A. Swenson, *J. Phys. Chem. Solids*, **24**, 1405 (1963).

(33) P. A. Bezuglyi, L. M. Tarasenko and O. L. Baryshevakii,

Sov. Phys. Solid State, **13**, 2003 (1971).
(34) T. H. K. Barron and M. L. Klein, *Proc. Phys. Soc.*, **82**, 161 (1973); **85**, 523 (1965).
(35) H. R. Glyde, *J. Phys.*, **C3**, 810 (1970).
(36) (a) R. H. Beaumont, H. Chihara and J. A. Morrison, *Proc. Phys. Soc.*, **78**, 1462 (1961); (b) P. Flubacher, A. J. Leadbetter, J. A. Morrison, *ibid.*, **78**, 1449 (1961).

The Transport Phenomena of a Series of Amides through the Copolymer Hydrogel Membranes

Hyeon Sook Koo* and Mu Shik Jhon

Korea Advanced Institute of Science, P.O. Box 150, Cheong Ryang Ri, Seoul 131, Korea
(Received October 8, 1980)

Hydrogel membranes were prepared by copolymerizing 2-hydroxyethyl methacrylate (HEMA) and N-vinyl-2-pyrrolidone (VP) in the presence of the solvent and the crosslinker tetraethyleneglycol dimethacrylate (TEGDMA). By changing the monomer composition and the crosslinker content, different membranes were synthesized. Using these membranes, relative permeabilities and distribution coefficients for amides including urea were measured. The water contents in membrane were also measured. On the basis of solute-membrane matrix interaction, the results were interpreted.

1. Introduction

Hydrogels are three dimensional networks of hydrophilic polymers, generally covalently or ionically crosslinked, which interact with aqueous solutions by swelling to be some equilibrium value. Because of high water contents, hydrogels are biocompatible, and used as materials of contact lenses, artificial kidney, and so forth.[1] Poly(HEMA) is the most widely used hydrogel and can be applied as a material for hemodialysis.[2] Uncrosslinked poly(VP) is extremely soluble in water and high concentrations of crosslinker (5-20%) are needed to produce a material with useful mechanical properties. Faster metabolic water transfer was obtained with diisocyanate crosslinker poly(VP) than the conventional cellulosic membranes.[3]

The transport phenomena through some poly(HEMA) membranes have been previously investigated.[4-6] Yasuda *et al.*[4,7] have analyzed the diffusion data, based on the free volume theory, for homogeneous hydrogel membranes.

With varying crosslinker concentration and water content, Wisniewski *et al.*[8] obtained diffusion data, which provided the additional information on the basic transport mechanisms for water in hydrogels and on the role of water in the transport of other solutes. Two basic mechanisms are the followings; 1) a microporous type membrane, which can act as a sieve with the solute molecules being transported through the minute pores of the membrane, and 2) a partition type, which further acts to slow the diffusion process due to the interaction between diffusing solute and membrane matrix or membrane water.

Lee *et al.*[9] investigated amide transport through poly(HEMA) membranes with varying crosslinker content. In the low crosslinker contents, the membrane behaves as pore type, and a linear relationship exists between molecular weight and relative permeability.

With increasing crosslinker content, the membrane behaves as partition type and the relationship is broken. In the partition membrane, urea has higher permeability, because urea with two amide groups has more hydrophilic interaction with the polymer matrix.

Transport of urea through hydrogel membranes was experimented in order to develop more efficient hemodialysis membranes.[2,3,10,11]

We investigated how crosslinker content and monomer composition affected the diffusion data, and compared with Lee *et al.*'s.

2. Theory

Relative Permeability. The equation used to obtain permeability U was derived elsewhere.[12]

$$\ln\left(\frac{2C_t}{C_0} - 1\right) = -U \cdot S \cdot \frac{2t}{V_1} \qquad (1)$$

where C_t, C_0, S and V_1 are the concentration at time, t, that at time 0, the surface area of membrane exposed to both solution, and the cell compartment volume, respectively.

* Present Address: Korea Atomic Energy Research Institute, Seoul, Korea.